Laser control of a multilevel quantum system as static parameter optimization with the help of effective decomposition

M. Sugawara

Department of Fundamental Science and Technology, Graduate School of Science and Technology, Keio University, 3-14-1 Hiyoshi, Kohoku-ku, Yokohama 223-8522, Japan

(Received 27 October 2009; published 22 January 2010)

A quantum control scheme for multilevel systems utilizing effective decomposition is proposed. In this method, a subsystem chosen for control target is effectively isolated by irradiating intense continuous-wave laser fields onto the complimentary space. By choosing the control target space consisting of small number of eigenstates, effective dressed states for the isolated space are analytically given, which makes it possible to express the performance index defined in the target space as an explicit function of laser parameters. Then, designing the control field can be treated as a static parameter optimization. The present scheme makes it possible not only to optimize the laser parameters but also to investigate the parameter search space, which clarifies the physics of the control process.

DOI: 10.1103/PhysRevA.81.013410 PACS number(s): 32.80.Qk, 42.50.Hz

I. INTRODUCTION

Coherent control of chemical reactions using external laser fields has been an active research area for a number of years [1–7]. Among various coherent control theories proposed so far, the most general purpose oriented methods for designing the control field are optimal control theory (OCT) [2,4,8] and local control theory (LCT) [3,5–7], which are based on the control theories. These methods require time-consuming numerical integration to obtain the system dynamics at every evaluation of the performance or cost index. Moreover, OCT requires such numerical integration during the iterative procedure. Thus, the application of these powerful general approaches becomes difficult as the system becomes realistic with numbers of eigenstates, because the time evolution of the whole system under the control field should be numerically calculated in both approaches.

On the other hand, we have shown that arbitrary multilevel systems can be effectively decomposed into isolated subspaces by irradiating intense continuous-wave (CW) lasers [9,10]. In these studies, a multilevel quantum system is decomposed into two subspaces, called P and Q spaces. Here, P space consists of eigenstates for control target, whereas Q space is defined as its compliment space. Irradiating intense CW lasers tuned to the transitions in the Q space makes it possible to exclude the Q space from the system dynamics or isolate the P space effectively. In the former studies, we succeeded in applying well-established control schemes such as π pulse [11] and STIRAP [12–15] to the P subspace.

In this study, we especially focus on the fact that one can obtain the P space dressed eigenstates analytically by choosing very small P space, i.e., consisting of a few levels. Using those dressed states, one can obtain the performance or cost index as an explicit function of laser parameters, that is defined for evaluating the current quantum state. Once we obtain such a performance or cost index, we can apply general optimization methods with respect to the laser parameters avoiding time-consuming numerical integration of the Schrödinger equation. This should be a significant advantage over the direct application of the OCT/LCT to the whole system because numerical integrations. We apply the above control scheme to a model system with double-well potential and show its usefulness.

II. THEORETICAL

We briefly summarize the effective decomposition scheme developed in the previous work [9,10]. Consider a general multilevel system as shown in Fig. 1. Now, we formally split the system into two subspaces, which we call P and Q consisting of N and M states, respectively, i.e., $\{|P_1\rangle, |P_2\rangle, \ldots, |P_N\rangle\}$ and $\{|Q_1\rangle, |Q_2\rangle, \ldots, |Q_M\rangle\}$. We define the P space so that there exist no direct optical transitions within the space, while the Q-space states are strongly coupled through the intense system-field interactions $\{\Omega_{ij}\}$. The interspace optical interactions are denoted by $\{V_k\}$. We restrict consideration to linkage patterns in which all carrier frequencies are detuned by the same amount, Δ, from their respective resonance frequencies.

We start from a Green function form of the Schrödinger equation given as

$$(z - \hat{H}) \cdot \hat{G}(z) = \hat{1}, \tag{1}$$

where $\hat{H}$ is the total Hamiltonian. Here, we set $\hbar = 1$ for simplicity. The Green function of the total system, $\hat{G}(z)$, is related to the time-evolution operator $\hat{U}(t)$ as

$$\hat{G}(z) = -i \int_0^\infty \hat{U}(t) e^{-izt} dt. \tag{2}$$

Applying the projection operator method onto Eq. (1) gives the P-space Green function $\hat{G}_P(z) \equiv \hat{P}\hat{G}(z)\hat{P}$ as

$$\hat{G}_P(z) = \frac{1}{z - \hat{H}_P(z)}, \tag{3}$$

where

$$\hat{H}_P(z) \equiv \Delta \hat{I}_P - \hat{P}\hat{H}\hat{Q}(z - \hat{Q}\hat{H}\hat{Q})^{-1}\hat{Q}\hat{H}\hat{P}. \tag{4}$$

Here, $\hat{P}$ and $\hat{Q}$ are the projection operators with respect to the P and Q spaces, respectively. Note that $\hat{P}H\hat{P}$ can be replaced with $\Delta\hat{I}_P$, where $\hat{I}_P$ is the identity operator for the P space.

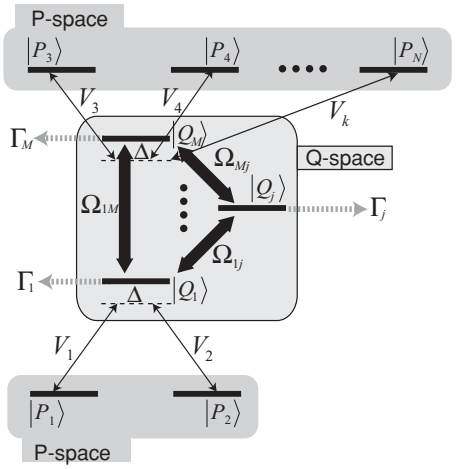

FIG. 1. Schematic diagram of P-Q space separation for a general multilevel quantum system.

Under the special condition, $V_k \ll \Omega_{ij}$ for arbitrary i, j, k, Eq. (4) can be approximated as $\hat{H}_P(\Delta)$ [9,10,16]. This implies that P space is effectively isolated and one can regard $\hat{H}_P(\Delta)$ as an effective Hamiltonian that governs the P-space dynamics. In such a case, P-space dynamics can be systematically investigated by the eigenvalue-state analysis, i.e., by solving the time-independent Schrödinger equation

$$\hat{H}_P(\Delta)|\phi_m\rangle = E_m|\phi_m\rangle. \tag{5}$$

For a dissipative system, eigenvalue E_m can be a complex value as $E_m = \epsilon_m - i\Gamma_m$, while ϵ_m and Γ_m are both real.

Here, we expand the initial state $|\Psi(0)\rangle$ and the target state $|\Psi_T\rangle$ in the eigenstates $\{|\phi_m\rangle\}$ as

$$|\Psi(0)\rangle = \sum_m c_m|\phi_m\rangle, \tag{6}$$

$$|\Psi_T\rangle = \sum_m d_m|\phi_m\rangle. \tag{7}$$

For applying the OCT, we define two types of performance indices, $I(t)$ and $J(T)$ as follows. The first one, $I(t)$, is defined locally in time as

$$I(t) = |\langle\Psi_T|\Psi(t)\rangle|^2 = |\langle\Psi_T|e^{-i\hat{H}_P t}|\Psi(0)\rangle|^2 = \left|\sum_m d_m^* c_m e^{-i\epsilon_m t-\Gamma_m t}\right|^2, \tag{8}$$

which denotes how much the current state $|\Psi(t)\rangle$ overlaps with the target state $|\Psi_T\rangle$. Another performance index, $J(T)$, is defined as a time-averaged $I(t)$ over a given time-duration T as

$$J(T) = \frac{1}{T}\int_0^T I(t)dt = \sum_{\Gamma_m=0}|d_m|^2|c_m|^2 + \frac{1}{2\Gamma_m T}\sum_{\Gamma_m\neq 0}|d_m|^2|c_m|^2(1-e^{-2\Gamma_m}) - \frac{i}{T}\sum_{m\neq n} d_m^* d_n c_m c_n^*\left(\frac{1-e^{-i\epsilon_{mn}T-\Gamma_{mn}T}}{\epsilon_{mn}-i\Gamma_{mn}}\right), \tag{9}$$

where $\epsilon_{mn} \equiv \epsilon_m - \epsilon_n$ and $\Gamma_{mn} = \Gamma_m + \Gamma_n$. Note that $I(t)$ and $J(t)$ correspond to the performance or cost indices defined in LCT and OCT, respectively.

If we choose the P system so that it consists of very small number of eigenstates, such as two or three, we can obtain the eigenstates $\{|\phi_m\rangle\}$ and eigenvalues E_m analytically. Using these analytical expressions, the performance indices $I(t)$ and $J(T)$ can be readily given as a explicit function of laser parameters. Then, the laser optimization turns out to be the static nonlinear parameter optimization problem with respect to $I(t)$ or $J(T)$.

III. APPLICATION

We consider a one-dimensional model system with a double-well potential as shown in Fig. 2. Such a potential curve is used to describe chemical reaction, for example, ring puckering isomerization [5]. The eigenstates localized in the right and left well, $|P_1\rangle$ and $|P_2\rangle$, correspond to different isomers, respectively. In the case that the initial state is taken to be $|P_1\rangle$, the coherent control of the isomerization is realized by promoting the optical transition from $|P_1\rangle$ to $|P_2\rangle$. In the present case, one can hardly make the direct optical transition $|P_1\rangle \leftrightarrow |P_2\rangle$ occur since there is very little transition dipole moment due to small overlap between those eigenfunctions. Thus, one needs to utilize the delocalized intermediate state, for example $|Q_1\rangle$, which can be optically accessible from both the initial and the target states. However, excited intermediates states often possesses dissipative nature due to the couplings to other vibrational modes or environment. Here, we take into account the dissipative nature of $|Q_1\rangle$ by introducing the imaginary part of the eigenvalue, Γ_1.

To see how the system suffers from the dissipation of $|Q_1\rangle$, we set up the model system with three states, $|P_1\rangle$, $|Q_1\rangle$, and $|P_2\rangle$. We apply two resonant CW lasers corresponding to $|P_1\rangle \leftrightarrow |Q_1\rangle$ and $|Q_1\rangle \leftrightarrow |P_2\rangle$ transitions with the interaction amplitude V_1 and V_2, respectively. The total Hamiltonian under the rotating wave approximation is given as

$$\mathbf{H} = \begin{pmatrix} 0 & 0 & V_1 \\ 0 & \Delta & V_2 \\ V_1 & V_2 & -i\Gamma_1 \end{pmatrix}. \tag{10}$$

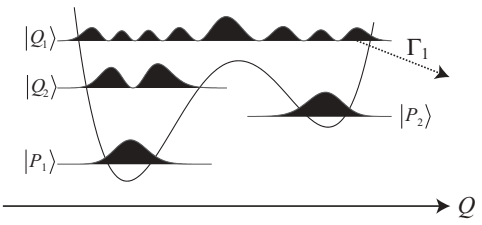

FIG. 2. Example of one-dimensional double-well model potential system. Square of several eigenfunctions are drawn together with the potential curve. Horizontal axis Q denotes the abstract reaction coordinate and the lines on which eigenfucntions are drawn represents the eigenenergies, respectively.

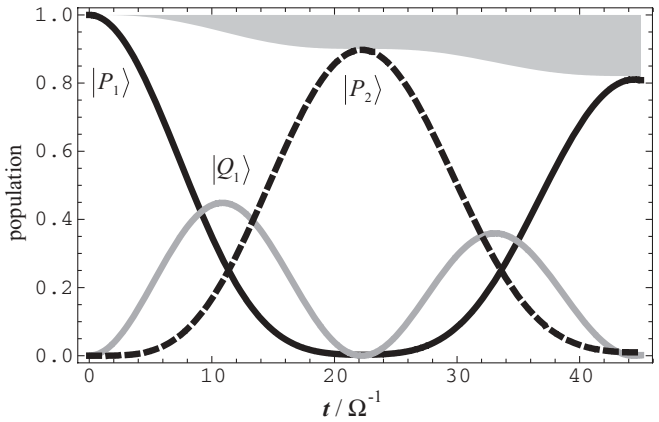

FIG. 3. Population dynamics of the three-level system consisting of $|P_1\rangle$, $|Q_1\rangle$, and $|P_2\rangle$. Parameters are taken to be $\delta = 0$, $\lambda_1 = \lambda_2 = 1$, $\gamma_1 = 0.01$. Solid, gray, and broken lines denote the population dynamics of $|P_1\rangle$, $|Q_1\rangle$, and $|P_2\rangle$, respectively. The area with light gray denotes the population lost due to the dissipation of $|Q_1\rangle$.

For simplicity, we redefine the total Hamiltonian in a nondimensional form as

$$\mathbf{H} = \begin{pmatrix} 0 & 0 & \lambda_1 \\ 0 & \delta & \lambda_2 \\ \lambda_1 & \lambda_2 & -i\gamma_1 \end{pmatrix}. \tag{11}$$

by measuring the energy in a unit of Ω where $\delta \equiv \Delta/\Omega$, $\gamma_i \equiv \Gamma_i/\Omega, \lambda_i \equiv V_i/\Omega$. Note also that corresponding unit time is Ω^{-1} throughout this study.

Shown in Fig. 3 is the population dynamics with the laser parameters $\lambda_1 = 1$, $\lambda_2 = 1$, $\delta = 0$, and $\gamma_1 = 0.01$. For example, in the case of Ref. [5], these parameters correspond to the actual laser amplitude 1.28×10^{10} V/m. Here, vibrational dissipation is estimated as $\Gamma \sim 10^{-5}$ atomic units (a.u.) and the dipole moments of relevant transitions are taken to be 0.4 a.u. As shown in Fig. 3, the population transfers from $|P_1\rangle$ to the target state $|P_2\rangle$ at $t = 22$ via the intermediate state $|Q_1\rangle$. However, 10% of the total population is lost during the optical process (see the gray-filled area in Fig. 3). This implies that the naive introduction of the dissipative intermediate state $|Q_1\rangle$ leads to considerable decreasing of the final yield.

Now, we consider utilizing a helper state to avoid population loss due to the dissipative dynamics. We choose the state $|Q_2\rangle$ localized in the left well (see Fig. 2) as a helper state. Note that we suppose $|Q_2\rangle$ has no dissipative nature with real eigenvalue. Then, we can construct four-level system, consisting of $|P_1\rangle$, $|P_2\rangle$, $|Q_1\rangle$, $|Q_2\rangle$, whose total Hamiltonian matrix is given as

$$\mathbf{H} = \begin{pmatrix} \delta & 0 & \lambda_1 & 0 \\ 0 & \delta & \lambda_2 & 0 \\ \lambda_1 & \lambda_2 & -i\gamma_1 & 1 \\ 0 & 0 & 1 & 0 \end{pmatrix}. \tag{12}$$

From Eq. (4), we obtain the matrix representation of $\hat{H}_P(z)$ as

$$\hat{\mathbf{H}}_P(z) = \begin{pmatrix} \delta & 0 \\ 0 & \delta \end{pmatrix} - \frac{z}{D_Q(z)} \begin{pmatrix} \lambda_1^2 & \lambda_1\lambda_2 \\ \lambda_1\lambda_2 & \lambda_2^2 \end{pmatrix}, \tag{13}$$

where $D_Q(z) = 1 - z(z - i\gamma_1)$. The effective Hamiltonian matrix defined in the limit of small λ, is given as

$$\mathbf{H}_{\text{eff}} = \tilde{\mathbf{H}}_P(\delta) = \begin{pmatrix} \delta & 0 \\ 0 & \delta \end{pmatrix} - \frac{\delta}{D_Q(\delta)} \begin{pmatrix} \lambda_1^2 & \lambda_1\lambda_2 \\ \lambda_1\lambda_2 & \lambda_2^2 \end{pmatrix}. \tag{14}$$

Diagonalizing the effective Hamiltonian, one obtains the eigenvalues, ϵ_1 and ϵ_2

$$\epsilon_1 = \delta - \frac{\delta\left(\lambda_1^2 + \lambda_2^2\right)}{D_Q(\delta)}, \tag{15}$$

$$\epsilon_2 = \delta, \tag{16}$$

and corresponding eigenvectors

$$|\phi_1\rangle : \frac{1}{\sqrt{\lambda_1^2 + \lambda_2^2}} \begin{pmatrix} \lambda_1 \\ \lambda_2 \end{pmatrix}, \tag{17}$$

$$|\phi_2\rangle : \frac{1}{\sqrt{\lambda_1^2 + \lambda_2^2}} \begin{pmatrix} -\lambda_2 \\ \lambda_1 \end{pmatrix}. \tag{18}$$

Substituting Eqs. (15), (16), (17), and (18) into Eqs. (8) and (9) gives a fully analytical expression of the performance indices, $I(t)$ and $J(T)$.

Now, we investigate the laser parameter dependence of $I(t)$. Shown in Fig. 4(a) is the (λ_1, λ_2) dependence of $I(t)$ while other parameters are fixed to be $\delta = 0.1$, $\gamma_1 = 0.01$, and $t = 5000$. There are regularly repeated ridges along the arc lines with a certain radius. Such a property of the search space can be understood by considering the system dynamics as follows. Since the P space is isolated as a two-level system under the CW-laser field, its dynamics is basically characterized by Rabi oscillations [11]. From the eigenvalues, Eqs. (15) and (16) and $D_Q(\delta) \approx 1$, the period of Rabi oscillation T_R is approximately given as

$$T_R = \frac{2\pi}{\delta\left(\lambda_1^2 + \lambda_2^2\right)}. \tag{19}$$

Since the total population oscillates between $|P_1\rangle$ and $|P_2\rangle$ with the period T_R, the target state population takes maximum values at $t = (n + 1/2)T_R$ with $n = 0, 1, 2, \ldots$. Thus, for the fixed t, $I(t)$ takes maximum values when the specific condition $(n + 1/2)T_R = t$, or

$$\left(n + \frac{1}{2}\right) \frac{2\pi}{\delta\left(\lambda_1^2 + \lambda_2^2\right)} \approx t \tag{20}$$

is satisfied, which creates the ripples in Fig. 4(a). Every ridge line satisfies the condition $\lambda_1^2 + \lambda_2^2 = \text{const}$. On each ridge, $I(t)$ takes maximum value when $\lambda_1 = \lambda_2$. This is because of the structure of the effective Hamiltonian, Eq. (14), that is, λ_1^2 and λ_2^2 are at diagonal elements. The difference between λ_1 and λ_2 corresponds to "effective" detuning in the isolated P space. Thus, as the difference between λ_1 and λ_2 increases, the amplitude of the Rabi frequency becomes small because of the detuning effect, which leads to low $I(t)$ value compared to the case, $\lambda_1 = \lambda_2$.

Shown in Fig. 4(b) is the (λ_1, λ_2) dependence of $J(T)$ while other parameters are taken to be the same as Fig. 4(a), i.e., $\delta = 0.01$, $\gamma_1 = 0.01$. Note that $J(T)$ is obtained through the integration during $t = 0 \sim 5000$. The steepness of $I(t)$ surface

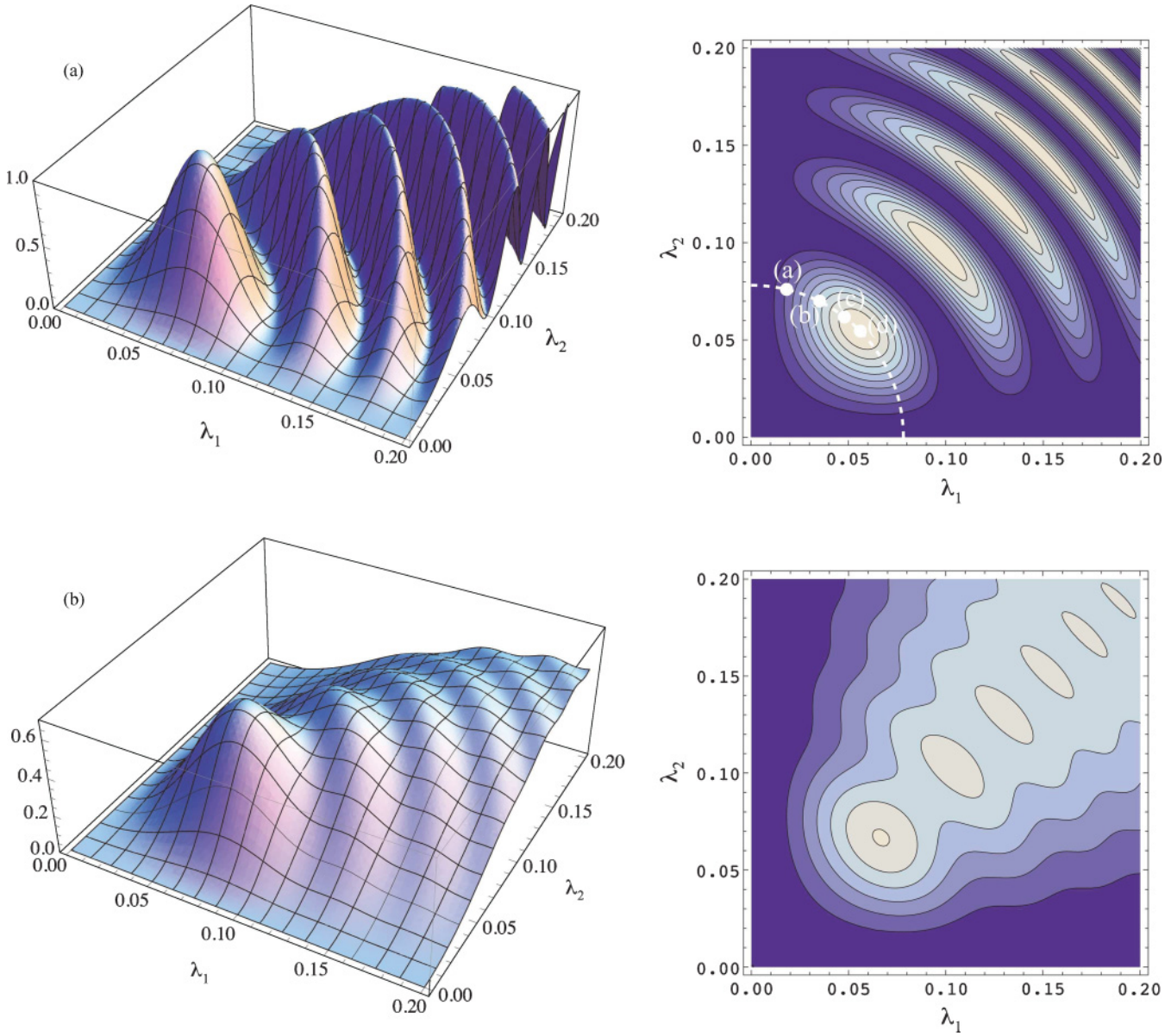

FIG. 4. (Color online) (λ_1, λ_2) dependence of $I(t)$ and $J(T)$ for the P space isolated from the 4-level system consisting of $|P_1\rangle$, $|P_2\rangle$, $|Q_1\rangle$, and $|Q_1\rangle$. (a) (λ_1, λ_2) dependence of $I(5000)$. Other parameters are fixed to be $\delta = 0$, 1, $\gamma_1 = 0.01$. (b) (λ_1, λ_2) dependence of $J(5000)$. Other parameters are fixed to be $\delta = 0$, 1, $\gamma_1 = 0.01$.

shown in Fig. 4(a) is smoothed through the time-averaging integration. Note that the damping of the oscillation along the $\lambda_1 = \lambda_2$ line is also due to the averaging process and is not from the population loss due to Γ_1.

We have performed a numerical search for the optimal parameter set at around the first peak corresponding to the smallest Rabi frequency in Fig. 4(a) and obtained the optimal values, $\lambda_1 = \lambda_2 = 0.056$, which corresponds to the actual laser amplitude setting 1×10^9 V/m for the interaction Ω and 1×10^7 V/m for the interaction V_k $(k = 1, 2)$, respectively, in the case of Ref. [5]. However, the parameter search turns out to be difficult as the Rabi frequency becomes large because of the complicated feature of the search space with numerous local minima as shown in Fig. 4(a). Comparing Figs. 4(a) and 4(b), one can tell that $J(T)$ surface is more suitable for numerical optimization in the OCT because its behavior is more moderate than $I(t)$ and it is likely not to fall in the local minima during the global optimization process.

Shown in Fig. 5 are the population dynamics in the P space changing the ratio, $\lambda_1/\lambda_2 (= V_2/V_1)$. The quantity $\lambda_1^2 + \lambda_2^2$ that determines the effective Rabi frequency is fixed to be $\pi/500$. These conditions correspond to the points shown as 5(a), 5(b), 5(c), and 5(d) on the contour plot of $I(t)$ in Fig. 4(a). The population is completely transferred when $\lambda_1 = \lambda_2 = 0.056$ [see Fig. 5(d)], which corresponds to the effective resonant condition. On the other hand, as shown in Figs. 5(a)–5(c) the maximum population of the target state does not reach to unity due to the effective detuning condition, $\lambda_1 \neq \lambda_2$.

Shown in Fig. 6 is (λ, δ) dependence of $I(t)$, while $\lambda \equiv \lambda_1 = \lambda_2$. Other parameters are taken to be $t = 5000$ and $\gamma_1 = 0.01$. There are repeated ridge lines and the first one, that is specified with white thick white broken line corresponds

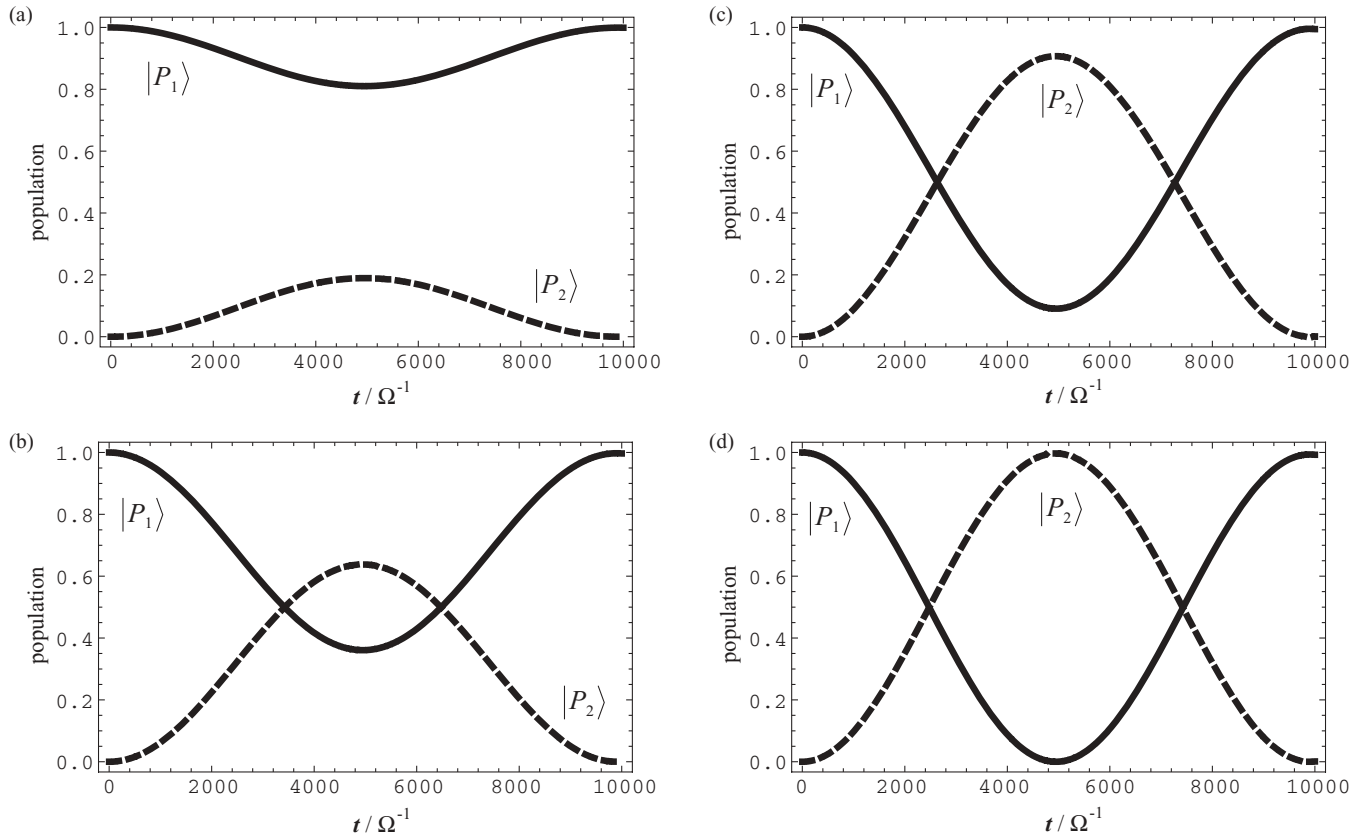

FIG. 5. Population dynamics of $|P_1\rangle$ and $|P_2\rangle$ in P space, changing λ_1/λ_2, whereas $\lambda_1^2 + \lambda_2^2$ is fixed to be $\pi/250$. Other parameters are taken to be $\delta = 0.1$, $\gamma_1 = 0.01$. Solid and broken lines denote the population dynamics of $|P_1\rangle$, and $|P_2\rangle$, respectively. λ_1, λ_2 are taken as follows: (a) $\lambda_1 = 0.018$, $\lambda_2 = 0.077$; (b) $\lambda_1 = 0.035$, $\lambda_2 = 0.071$; (c) $\lambda_1 = 0.047$, $\lambda_2 = 0.064$; (d) $\lambda_1 = 0.056$, $\lambda_2 = 0.056$.

to the condition in which the final time $t = 5000$ corresponds to half a cycle of the Rabi oscillation, i.e., π-pulse situation. Note that all the parameter sets on this ridge line correspond to the dynamics which realizes almost 100% population transfer to the target state. In such a case, direct OCT application to the original four-level system together with gradient based numerical optimization faces serious difficulties in finding optimal values because of very small gradient along those ridge lines shown in Fig. 6.

Here, we discus applicability of the present method to pulse shaping problems. Although the formulation of the present scheme is based on the system Hamiltonian under the CW-laser conditions, it can be used for designing the pulse envelope under limited conditions as follows. For simplicity, we consider two-level system dynamics under resonant pulse laser with envelope function $f(t)$ and interaction amplitude Ω_0. Assuming that RWA approximation is valid, the Schröringer equation is given as

$$\frac{d}{dt}\begin{pmatrix} c_1(t) \\ c_2(t) \end{pmatrix} = -\frac{i}{2}\begin{pmatrix} 0 & \Omega_0 f(t) \\ \Omega_0 f(t) & 0 \end{pmatrix}\begin{pmatrix} c_1(t) \\ c_2(t) \end{pmatrix}. \quad (21)$$

Here, we define the new variable τ, which is a function of t as

$$\tau(t) = \int_0^t dt' f(t'). \quad (22)$$

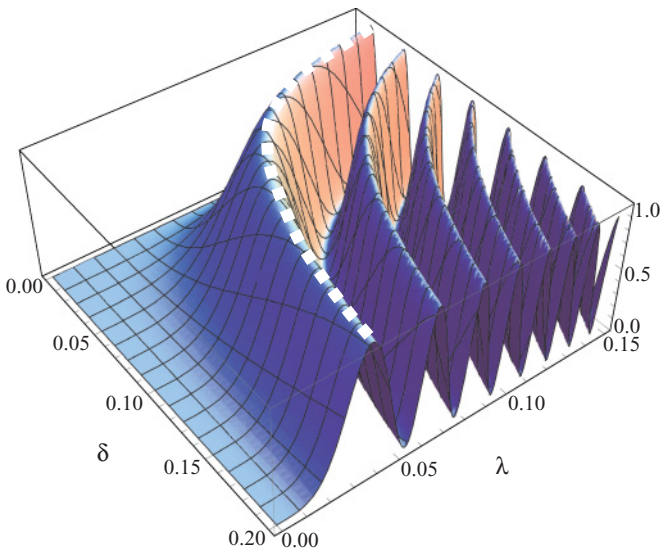

FIG. 6. (Color online) (δ, λ) dependence of $I(t)$ for the P space, which is isolated from the original four-level system consisting of $|P_1\rangle$, $|P_2\rangle$, $|Q_1\rangle$, and $|Q_1\rangle$. $\lambda \equiv \lambda_1 = \lambda_2$ and other parameters are fixed to be $\gamma_1 = 0.01$, $t = 5000$.

Considering $c_i(t)$ as a function τ, $\tilde{c}_i(\tau)$, we rewrite Eq. (21)

$$\frac{d\tau}{dt}\frac{d}{d\tau}\begin{pmatrix}\tilde{c}_1(\tau)\\ \tilde{c}_2(\tau)\end{pmatrix} = f(t)\frac{d}{d\tau}\begin{pmatrix}\tilde{c}_1(\tau)\\ \tilde{c}_2(\tau)\end{pmatrix} = -\frac{if(t)}{2}\begin{pmatrix}0 & \Omega_0\\ \Omega_0 & 0\end{pmatrix}\begin{pmatrix}\tilde{c}_1(\tau)\\ \tilde{c}_2(\tau)\end{pmatrix}, \quad (23)$$

which leads to

$$\frac{d}{d\tau}\begin{pmatrix}\tilde{c}_1(\tau)\\ \tilde{c}_2(\tau)\end{pmatrix} = -\frac{i}{2}\begin{pmatrix}0 & \Omega_0\\ \Omega_0 & 0\end{pmatrix}\begin{pmatrix}\tilde{c}_1(\tau)\\ \tilde{c}_2(\tau)\end{pmatrix}. \quad (24)$$

This is formally identical to the original equation of motion, Eq. (21). Thus, the static optimization scheme in the present method can be used to design the laser pulse for controlling $\tilde{c}_i(\tau)$. Since one can define the pulse area constant as $\tau(\infty)$ for an arbitrary laser pulse, pulse shaping problems can be dealt as a static optimization problem with respect to $\tilde{c}_i(\tau(\infty))$. Note that the $\tilde{c}_i(\tau)$ does not depend on the pulse envelope $f(t)$ but on τ, which implies that the system finally reach to the state $[\tilde{c}_1(\tau(\infty)), \tilde{c}_2(\tau(\infty))]^T$ irrelevant to actual shape of $f(t)$. One can extend the above formulation to multilevel systems as far as we take the same $f(t)$ for all laser pulses introduced and RWA stands. However, one should note that it is difficult to apply the present method to more flexible pulse designing, in which each pulse has different pulse envelope.

Lastly, we should mention the potential applicability to more realistic molecular system, in which there are numerous background states. If those background states are placed in the Q space and only single doorway state is coupled to those background states, the dissipative dynamics or population flow to the Q space can be suppressed by the present scheme. The application of the present scheme to the suppression of intramolecular vibrational energy redistribution (IVR) is now under study and will be reported elsewhere.

It is also interesting to consider how the suppression effect of dissipation works on the molecular dynamics induced by intense laser fields, such as multiphoton dissociation of H_2^+ [17]. In the H_2^+ case, the photodissociation originates from the optical coupling between two electronic states which possess bound and dissociative potential curves, respectively. In order to use the present scheme, it is necessary to introduce the helper electronic state with bound potential curve and apply another intense CW laser which optically connects the dissociative and the helper state more closely than that between original two states responsible for photodissociation. Note also that, for quantitative analysis on suppression effect, one needs to carry out numerical calculations with the help of grid basis and complex coordinate method in order to take into account the Floquet-Siegert resonance rigorously, which might make the laser optimization difficult, consequently.

Finally, we should mention that one needs to pay attention to actual line width of dissipative state and possible laser power to estimate the suppression effect. For example, for suppressing IVR ($\Gamma \sim 10^{-6}$ a.u.) of typical molecule with transition moment of 1 D, the CW laser with the amplitude $\sim 10^8$ V/m is needed, while for more wider dissipation such as shape resonances ($\Gamma \sim 10^{-3}$ a.u.), one needs to prepare 10^{11} V/m.

IV. SUMMARY

We have proposed a quantum control scheme for multilevel systems, in which the laser optimization is converted into static parameter search problem. In the present method, instead of carrying out the numerical integration for obtaining the time evolution of full original system, we utilize the effective decomposition brought by intense CW lasers. By using this scheme, we, first, isolate the subspace consisting of control target states. Second, we solve the Schrödinger equation for the isolated subspace to obtain the analytical solution of eigenvalues/states in order to to express the performance index as an explicit function of laser parameters. Thus, we have succeeded to convert a general time-dependent control problem into a static nonlinear optimization problem. Moreover, it allows us to investigate detailed features of the search space, which is difficult in the case of direct application of OCT/LCT, in which the system dynamics is numerically solved.

ACKNOWLEDGMENTS

This research was supported, in part, by the Japan Society for the Promotion of Science (JSPS), Grant-in-Aid for Scientific Research(C), KAKENHI(20550021).

[1] M. Shapiro and P. Brumer, Rep. Prog. Phys. **66**, 859 (2003).
[2] H. Rabitz, R. de Vivie-Riedle, M. Motzkus, and K. Kompa, Science **288**, 824 (2000).
[3] Y. Ohtsuki, H. Kono, and Y. Fujimura, J. Chem. Phys. **109**, 9318 (1998).
[4] S. Shi and H. Rabitz, J. Chem. Phys. **92**, 364 (1990).
[5] M. Sugawara and Y. Fujimura, J. Chem. Phys. **100**, 5646 (1994).
[6] M. Sugawara, J. Chem. Phys. **118**, 6784 (2003).
[7] A. Bartana and R. Kosloff, J. Chem. Phys. **99**, 196 (1993).
[8] Y. Ohtsuki, M. Sugawara, H. Kono, and Y. Fujimura, Bull. Chem. Soc. Jpn. **74**, 1167 (2001).
[9] M. Sugawara, M. Tamaki, and S. Yabushita, J. Phys. Chem. A **111**, 9446 (2007).
[10] M. Sugawara, J. Chem. Phys. **130**, 094103 (2009).
[11] P. Knight and P. Milonni, Phys. Rep. **66**, 21 (1980).
[12] Y. Ohta, T. Yoshimoto, T. Bando, H. Kizu, H. Nagao, and K. Nishikawa, Int. J. Quantum Chem. **80**, 1068 (2000).
[13] K. Nishikawa, T. Yamaguchi, I. Sakamoto, K. Nishi, Y. Ohta, and H. Nagao, Synth. Met. **137**, 1437 (2003).
[14] V. Kurkal and S. A. Rice, J. Phys. Chem. B **105**, 6488 (2001).
[15] K. Bergmann, H. Theuer, and B. Shore, Rev. Mod. Phys. **70**, 1003 (1998).
[16] H. Tang, R. Kosloff, and S. A. Rice, J. Chem. Phys. **104**, 5457 (1996).
[17] R. Lefebvre, O. Atabek, M. Sindelka, and N. Moiseyev, Phys. Rev. Lett. **103**, 123003 (2009).